

1 **Rapidly predicting vancomycin resistance of *Enterococcus faecium* through**  
2 **MALDI-TOF MS spectrum obtained in real-world clinical microbiology**  
3 **laboratory**

4

5 Hsin-Yao Wang, MD<sup>1,2</sup>, Ko-Pei Lu, MS<sup>3</sup>, Chia-Ru Chung, MS<sup>4</sup>, Yi-Ju Tseng, PhD<sup>1,5</sup>, Tzong-  
6 Yi Lee, PhD<sup>1,6,7</sup>, Jorng-Tzong Horng, PhD<sup>1,4,8</sup>, Tzu-Hao Chang, PhD<sup>9,10</sup>, Min-Hsien Wu,  
7 PhD<sup>11,12,13</sup>, Ting-Wei Lin, MD<sup>1</sup>, Tsui-Ping Liu, MS<sup>1</sup>, Jang-Jih Lu, MD, PhD<sup>1,14,15\*</sup>

8

9 1. Department of Laboratory Medicine, Chang Gung Memorial Hospital at Linkou,  
10 Taoyuan City, Taiwan

11 2. Ph.D. Program in Biomedical Engineering, Chang Gung University, Taoyuan City,  
12 Taiwan

13 3. Graduate Program in Biomedical Information, Yuan-Ze University, Taoyuan City,  
14 Taiwan

15 4. Department of Computer Science and Information Engineering, National Central  
16 University, Taoyuan City, Taiwan

17 5. Department of Information Management, Chang Gung University, Taoyuan City,  
18 Taiwan

19 6. School of Science and Engineering, The Chinese University of Hong Kong, Shenzhen,  
20 China

21 7. Warshel Institute for Computational Biology, The Chinese University of Hong Kong,  
22 Shenzhen, China

23 8. Department of Bioinformatics and Medical Engineering, Asia University, Taichung  
24 City, Taiwan

25 9. Graduate Institute of Biomedical Informatics, Taipei Medical University, Taipei City,  
26 Taiwan

27 10. Clinical Big Data Research Center, Taipei Medical University Hospital, Taipei City,  
28 Taiwan.

29 11. Graduate Institute of Biomedical Engineering, Chang Gung University, Taoyuan City,  
30 Taiwan

31 12. Division of Haematology/Oncology, Department of Internal Medicine, Chang Gung  
32 Memorial Hospital at Linkou, Taoyuan City, Taiwan

33 13. Biosensor Group, Biomedical Engineering Research Center, Chang Gung University,  
34 Taoyuan City, Taiwan

35 14. School of Medicine, Chang Gung University, Taoyuan City, Taiwan

36 15. Department of Medical Biotechnology and Laboratory Science, Chang Gung  
37 University, Taoyuan City, Taiwan

38 \*To whom correspondence should be addressed: JJ Lu

39

40 **Keywords:** Vancomycin-resistant *Enterococcus faecium* (VRE<sub>fm</sub>); Antibacterial drug  
41 resistance; Matrix-assisted laser desorption ionization time-of-flight (MALDI-TOF) mass  
42 spectrometry; Machine learning; Rapid detection

43

44

45 **CORRESPONDENCE:** Jang-Jih Lu, M.D., Ph.D.

46 Department of Laboratory Medicine, Chang Gung Memorial Hospital at Linkou

47 Department of Medical Biotechnology and Laboratory Science, Chang Gung University

48 5 Fu-Shing St. Kweishan

49 Taoyuan 333, Taiwan

50 **Abstract**

51 *Enterococcus faecium* is one of the leading pathogens in the world. In this study, we proposed  
52 a strategy to rapidly and accurately distinguish vancomycin-resistant *Enterococcus faecium*  
53 (VRE<sub>fm</sub>) and vancomycin-susceptible *E. faecium* (VSE<sub>fm</sub>) to help doctors correctly determine  
54 the use of vancomycin by a machine learning (ML)-based algorithm. A predictive model was  
55 developed and validated to distinguish VRE<sub>fm</sub> and VSE<sub>fm</sub> by analyzing MALDI-TOF MS  
56 spectra of unique *E. faecium* isolates from different specimen types. Firstly, 5717 mass spectra,  
57 including 2795 VRE<sub>fm</sub> and 2922 VSE<sub>fm</sub>, were used to develop the algorithm. And 2280 mass  
58 spectra of isolates, namely 1222 VRE<sub>fm</sub> and 1058 VSE<sub>fm</sub>, were used to externally validate the  
59 algorithm. The random forest-based algorithm demonstrated good classification performances  
60 for overall specimens, whose mean AUROC in 5-fold cross validation, time-wise validation,  
61 and external validation was all greater than 0.84. For the detection of VRE<sub>fm</sub> in blood, sterile  
62 body fluid, urinary tract, and wound, the AUROC in external validation was also greater than  
63 0.84. The predictions with algorithms were significantly more accurate than empirical  
64 antibiotic use. The accuracy of antibiotics administration could be improved by 30%. And the  
65 algorithm could provide rapid antibiotic susceptibility results at least 24 hours ahead of routine  
66 laboratory tests. The turn-around-time of antibiotic susceptibility could be reduced by 50%. In  
67 conclusion, a ML algorithm using MALDI-TOF MS spectra obtained in routine workflow  
68 accurately differentiated VRE<sub>fm</sub> from VSE<sub>fm</sub>, especially in blood and sterile body fluid, which  
69 can be applied to facilitate the clinical testing process due to its accuracy, generalizability, and  
70 rapidness.

71

## 72 **Introduction**

73 *Enterococcus* spp. is one of the leading pathogens in healthcare-associated infection.<sup>1</sup>  
74 Enterococcal infection could cause urinary tract infection, blood stream infection, and even  
75 mortality.<sup>2</sup> Until recently, vancomycin was virtually the only drug that could be consistently  
76 relied on for treating multidrug-resistant enterococcal infections<sup>3,4</sup>. Vancomycin-resistant  
77 *Enterococcus* (VRE) has led to heavy burden on healthcare worldwide since its first-time  
78 isolation.<sup>5,6</sup> *Enterococcus faecalis* and *E. faecium* are the 2 most commonly isolated  
79 *Enterococcus* spp. in clinical practice.<sup>1</sup> VRE *faecium* (VRE<sub>fm</sub>) has received considerably more  
80 attention than VRE *faecalis* (VRE<sub>fs</sub>) because most of the clinically isolated VRE is *E. faecium*  
81 in the recent decades<sup>4,7</sup> and VRE<sub>fm</sub> causes more severe infection than VRE<sub>fs</sub><sup>8,9</sup>. Early detection  
82 of vancomycin resistance is essential for successfully treating VRE<sub>fm</sub> infection.<sup>10</sup> Vancomycin  
83 could be discontinued, and antimicrobial agents could be replaced with other antibiotics (eg,  
84 linezolid and daptomycin) based on the laboratory results of vancomycin resistance<sup>11,12</sup>.  
85 Patients' prognosis could be improved and further drug resistance development could be  
86 avoided by using susceptible antibiotics.<sup>11</sup> However, typical tests in clinical microbiology  
87 laboratories, such as the minimal inhibitory concentration test or agar-diffusion test, fail to  
88 provide results for antibiotic susceptibility rapidly. The antibiotic susceptibility test (AST) of  
89 vancomycin is time-consuming, and the Clinical and Laboratory Standards Institute  
90 recommended a full 24 hours should be held for accurate detection of vancomycin resistance  
91 in enterococci.<sup>13</sup> This would considerably delay accurate prescription of antibiotics against *E.*  
92 *faecium*. Furthermore, prescribing antibiotics based on empirical prescription, without  
93 determining AST, would result in low effectiveness (approximately 50%), depending on the  
94 local epidemiology of VRE<sub>fm</sub>.<sup>12</sup> Thus, a new tool is needed to provide AST for VRE<sub>fm</sub> rapidly  
95 and accurately.

96 Recently, matrix-assisted laser desorption ionization time-of-flight (MALDI-TOF) mass  
97 spectrometry (MS) has become popular among clinical microbiology laboratories worldwide  
98 because of its reliability, rapidity, and cost-effectiveness in identifying bacterial species.<sup>14-16</sup> In  
99 addition to species identification, MALDI-TOF MS has been promising in other applications,  
100 such as strain typing or AST.<sup>17-19</sup> MALDI-TOF MS can generate massive data comprising  
101 hundreds of peak signals on the spectra.<sup>17,20</sup> The complex data of MALDI-TOF spectra are  
102 overwhelming to even an experienced medical staff.<sup>19</sup> Studies have attempted to identify the  
103 characteristic peak through visual inspection.<sup>21,22</sup> The results of the studies have been  
104 discordant, which has limited the clinical utility.<sup>23-25</sup>

105 Machine learning (ML) is a good analytical method for solving classification problems  
106 through identification of implicit data patterns from complex data.<sup>26</sup> The ML method  
107 outperforms traditional statistical methods because of its excellent ability to handle complex  
108 interactions between large amount of predictors and good performance in non-linear  
109 classification problems<sup>27</sup> ML has been successfully applied in several clinical fields.<sup>27-36</sup> Thus,  
110 the ML algorithm is especially appropriate for analyzing complex data such as MALDI-TOF  
111 spectra. However, to our knowledge, few studies have used ML in the analysis of MALDI-  
112 TOF spectra for rapidly reporting *VRE<sub>fm</sub>*, and the case numbers in these studies were  
113 insufficient, and so, ML algorithm generalization has been limited.<sup>37-39</sup> Moreover, to date, no  
114 study has validated AST prediction ML algorithms by using large real-world data.

115 In this study, we aimed to develop and validate a *VRE<sub>fm</sub>* prediction ML model by using  
116 consecutively collected real-world data from 2 tertiary medical centers (Chang Gung Memorial  
117 Hospital [CGMH], Linkou branch and CGMH, Kaohsiung branch). Using the largest MALDI-  
118 TOF spectrum clinical data to date, the ML algorithm could predict *VRE<sub>fm</sub>* accurately, rapidly,  
119 and in a ready-to-use manner based on the real-world evidence, which is more representative  
120 for clinical practice.<sup>40</sup> Moreover, we confirmed the robustness and generalization of the ML

121 algorithm through several validation methods, namely cross-validation, time-wise internal  
122 validations (unseen independent testing dataset classified according to time), and external  
123 validation (unseen independent testing dataset from another medical center). According to the  
124 real-world evidence-based validation, our VRE $fm$  prediction ML models are ready to be  
125 incorporated into routine workflow.

## 126 **Materials and methods**

### 127 **Data source**

128 We designed a novel machine learning approach which can improve accuracy of  
129 antibiotics administration and reduce the turn-around-time of antibiotics susceptibility test. We  
130 summarized the comparison between the machine learning approach and the traditional  
131 approach used in current clinical microbiology laboratory. We schematically illustrated the  
132 study design in Figure 1(b). The data used in this retrospective study was consecutively  
133 collected from the clinical microbiology laboratories of 2 tertiary medical centers in Taiwan,  
134 namely CGMH Linkou branch and CGMH Kaohsiung branch between January 1, 2013 and  
135 December 31, 2017. The clinical microbiology laboratories collected and processed all the  
136 routine specimens obtained from the hospitals. In total, 7997 *E. faecium* cases were identified  
137 and included in this study, whereas 5717 (VRE $fm$ : 48.89%) and 2280 (VRE $fm$ : 53.60%) cases,  
138 respectively, were obtained from Linkou and Kaohsiung branches of CGMH. The *E. faecium*  
139 strains were isolated from blood, urinary tract, sterile body fluids, and wound. The detailed  
140 description of specimen types is provided in eTable 1 in the Supplement. The study was  
141 approved by the Institutional Review Board of Chang Gung Medical Foundation (No.  
142 201900767B0). We followed the Standards for Reporting of Diagnostic Accuracy 2015<sup>41</sup> and  
143 the Transparent Reporting of a Multivariable Prediction Model for Individual Prognosis or  
144 Diagnosis reporting guidelines.<sup>42</sup>

145

## 146 **Definition of *E. faecium* and vancomycin susceptibility**

147 *E. faecium* was identified using MALDI-TOF spectra measured using a Microflex LT  
148 mass spectrometer and analyzed using Biotyper 3.1 (Bruker Daltonik GmbH, Bremen,  
149 Germany). A log score (generated through Biotyper 3.1) larger than 2 was used for confirming  
150 *E. faecium*.<sup>17-19</sup> We tested vancomycin susceptibility of *E. faecium* by using the paper disc  
151 method. The details of *E. faecium* identification and AST are given in the eMethods in the  
152 Supplement.

153

## 154 **MALDI-TOF mass spectrum data collection and preprocessing**

155 The details were described in the Supplements.

156

## 157 **Peak selection from MALDI-TOF mass spectra for model development**

158 We applied the embedded feature-selection method to select the most important peaks  
159 from MALDI-TOF mass spectra.<sup>43</sup> The peaks were ranked using the p-values of the chi-square  
160 test of homogeneity, which was employed to determine whether frequency counts were  
161 distributed identically across VRE<sub>fm</sub> and vancomycin-susceptible *E. faecium* (VSE<sub>fm</sub>).  
162 Preliminarily, we selected top 10 important peaks to plot a heat map based on the hierarchical  
163 clustering (eMethods in the Supplement). All the ranked peaks were incorporated in the model  
164 accordingly until the performance did not increase. Consequently, we could obtain the  
165 important peaks that were highly related to differentiation of VRE<sub>fm</sub> and VSE<sub>fm</sub> isolates.

166 For determining the number of peaks included in the ML models, we forwardly added  
167 them into the ML models and calculated the performance using accuracy as the metric. First,  
168 the predictor candidates were sorted in a descending order according to the importance score,  
169 and one predictive peak was added at a time into the ML models. On the basis of predictive  
170 peak composition, we used different algorithms, namely random forest (RF), support vector

171 machine (SVM) with a radial basis function kernel, and k-nearest neighbor (KNN) and applied  
172 5-fold cross validation (CV) in the data from the CGMH Linkou branch. The accuracies of the  
173 ML models were calculated to determine the adequate number of predictive peaks included in  
174 the models.

175

## 176 **Development and validation of VRE<sub>fm</sub> prediction models**

177 We aimed to develop and validate a robust VRE<sub>fm</sub> prediction model capable of  
178 detecting VRE<sub>fm</sub> earlier than the AST report. Three commonly used ML algorithms, namely  
179 RF, SVM with a radial basis function kernel, and KNN, were used for developing the VRE<sub>fm</sub>  
180 prediction model. These ML algorithms have demonstrated their successful applications (either  
181 classification or prediction) in clinical practice.<sup>17-19,27,28,35,36</sup> The details of these ML algorithms  
182 and model training processes are attached in the eMethods in the Supplement.

183 We thoroughly evaluated the performance and robustness of the VRE<sub>fm</sub> prediction  
184 models using 5-fold CV, time-wise internal validation, and external validation. Data from the  
185 CGMH Linkou branch were used for 5-fold CV and time-wise internal validation; by contrast,  
186 data from the CGMH Kaohsiung branch served as the unseen independent testing data for  
187 external validation. For 5-fold CV, data were randomly divided into 5 datasets. Each one of the  
188 5 datasets served as the testing dataset to evaluate the performance of the model developed by  
189 the other 4 datasets. In 5-fold CV, we obtained 5 measurements of metrics for evaluating the  
190 robustness of VRE<sub>fm</sub> prediction models. Moreover, to evaluate performance using  
191 prospectively collected data, we conducted time-wise internal validation: we used data  
192 collected between January 1, 2013 and December 31, 2016 as the training dataset for  
193 developing VRE<sub>fm</sub> prediction models, while data from January 1, 2017 to December 31, 2017  
194 served as the testing dataset. To test the generalizability of the models, we used data from the  
195 CGMH Linkou branch to develop VRE<sub>fm</sub> prediction models and used data from the CGMH

196 Kaohsiung branch to test the models' performance in a different institute. Additionally, we  
197 evaluated the performance of the *VRE<sub>fm</sub>* prediction model using different types of specimens,  
198 namely blood, urinary tract, sterile body fluid, and wound, by using data from the CGMH  
199 Kaohsiung branch. We adopted metrics including sensitivity, specificity, accuracy, positive  
200 predictive value (PPV), negative predictive value (NPV), receiver operating characteristic  
201 (ROC) curve, and area under the receiver operating characteristic curve (AUROC) to assess  
202 and compare the performance of the *VRE<sub>fm</sub>* prediction model.

203

## 204 **Statistical analysis**

205 The confidence intervals for sensitivity, specificity, and accuracy were estimated  
206 using the calculation of the confidence interval for a proportion in one sample situation.  
207 Specifically, the critical values followed the Z-score table. To compare the percentages in  
208 matched samples, Cochran's Q test, a nonparametric approach, was implemented in this  
209 study.<sup>44</sup> Then, we employed pairwise McNemar's tests<sup>45</sup> for post hoc analysis and adopted  
210 the false discovery rate proposed by Benjamini and Hochberg (1995) to adjust the *P* value.<sup>46</sup>  
211 Furthermore, the confidence intervals of AUROCs were determined using the nonparametric  
212 approach, and the AUROC comparisons mainly adopted the nonparametric approach  
213 proposed by DeLong et al.<sup>47</sup>

214

## 215 **Results**

### 216 **Predictive peaks for detecting *VRE<sub>fm</sub>***

217 We defined crucial predictive peaks when the occurrence frequency of a peak was  
218 significantly different (defined by the chi-square test) in *VRE<sub>fm</sub>* and *VSE<sub>fm</sub>*. In the step of  
219 extracting predictor candidates, 876 predictor candidates were extracted. From the predictor  
220 candidates, we used the chi-square method to select important predictive peaks.



221 We selected 10 most critical predictive peaks and plotted a heat map to preliminarily  
222 visualize the difference between *VREfm* and *VSEfm* (Figure 2). Peaks of  $m/z$  3172, 3302, 3645,  
223 6342, 6356, 6603, and 6690 were found more frequently in *VREfm*; by contrast,  $m/z$  3165,  
224 3681, and 7360 occurred more frequently in *VSEfm*. Although these important predictive peaks  
225 were statistically significant, we found them in both *VREfm* and *VSEfm*. The full list of crucial  
226 predictive peaks is provided in eTable 2 in the Supplement.

227 We selected several important predictive peaks from the predictor candidate list, which  
228 was ordered according to the chi-square score. eFigure 4 in the Supplement shows the change  
229 in ML models performance when the number of critical predictive peaks increased. For all the  
230 ML algorithms used in the study, a similar trend of performance was observed: the accuracies  
231 of the ML models reached a steady plateau when the included number of important predictive  
232 peaks was larger than 100 (eFigure 4 in the Supplement). Thus, the top 100 crucial predictive  
233 peaks were selected as the peak composition for the following experiments.

234

### 235 **Performance of *VREfm* prediction models**

236 We summarized the ML models' performance in Table 1, Table 2, and Figure 3. The  
237 details of comparison between different algorithms are described in the Supplement. The RF  
238 model outperformed SVM and KNN in 5-fold CV, time-wise internal validation, and external  
239 validation (eTable 3 in the Supplement), where the AUROC ranged from 0.8463 to 0.8553 and  
240 accuracy ranged from 0.7769 to 0.7855. Moreover, performance robustness was also observed  
241 in SVM and KNN. Figure 3 shows typical ROC curves for the 3 algorithms in all the 3  
242 validations. We used Youden's index to select the threshold from the ROC curves in search of  
243 balanced sensitivity and specificity. In external validation, the sensitivity and specificity of RF  
244 were 0.7791 (95% confidence interval: 0.7620-0.7961) and 0.7930 (95% confidence interval:

245 0.7764-0.8096). On the basis of the resistance rate (VRE<sub>fm</sub>: 53.60%) in the external validation  
246 dataset, the PPV was 0.8130 and the NPV was 0.7565.

247         Given that the RF algorithm attained the highest performance, additionally, we tested  
248 the performance of the RF-based VRE<sub>fm</sub> prediction model using different types of specimens  
249 in the independent testing dataset (ie, external validation by using data of the CGMH  
250 Kaohsiung branch) (Table 2). The RF-based VRE<sub>fm</sub> prediction model attained higher  
251 performance in predicting VRE<sub>fm</sub> in blood and sterile body fluid specimens than the other  
252 specimen types. The AUROC of blood specimens reached 0.9103 (95% confidence interval:  
253 0.8727-0.9480), whereas that of sterile body fluid specimens reached 0.8714 (95% confidence  
254 interval: 0.8321-0.9106). Moreover, the sensitivity (0.8870, 95% confidence interval: 0.8436-  
255 0.9303) and specificity (0.8000, 95% confidence interval: 0.7452-0.8548) of the RF-based  
256 VRE<sub>fm</sub> prediction model for the blood specimen were also balanced and significantly higher  
257 than those for other specimens. By contrast, the performance of the RF-based VRE<sub>fm</sub>  
258 prediction model for urinary tract specimens (0.8494, 95% confidence interval: 0.8258-0.8731)  
259 was similar to that for overall specimens (0.8553, 95% confidence interval: 0.8399-0.8706).

260

## 261 **Discussion**

262         We developed ML-based models for predicting VRE<sub>fm</sub> rapidly and accurately based  
263 on MALDI-TOF MS data. The models were especially effective in predicting VRE<sub>fm</sub> in  
264 invasive infections (ie, blood and sterile body fluid). We used the largest up-to-date real-world  
265 data to validate the robustness and generalization of the ML-based models by using k-fold CV,  
266 time-wise internal validation, and external validation. The rapid and accurate AST of  
267 vancomycin is promising for determining antibiotics against VRE<sub>fm</sub> infection.

268         Our results suggested that AST could be predicted accurately by using ML algorithms  
269 to analyze MALDI-TOF MS data. MALDI-TOF MS is a powerful analytical tool in current

270 clinical microbiology laboratories because of its rapidness and cost-effectiveness in identifying  
271 bacterial species.<sup>14-16</sup> On the basis of the massive data produced by MALDI-TOF MS,  
272 moreover, some studies have demonstrated that subspecies typing could be predicted from a  
273 specific pattern of MS spectra only.<sup>17,19</sup> Furthermore, other studies have shown a good  
274 correlation between AST and specific patterns of MS spectra.<sup>18,23-25,48</sup> However, some issues  
275 have limited the generalization of these results. First, most of the studies have adopted an  
276 additional protein extraction step before analytical measurement of MALDI-TOF MS. The  
277 protein extraction step could enhance data quality; however, it is not routinely used in clinical  
278 practice because it is labor-intensive, time-consuming, and expensive.<sup>17,18</sup> By contrast, we used  
279 the direct deposition method, which is recommended by the manufacturer and is used for  
280 everyday works. Thus, our models are more feasible for the existing workflow because they  
281 were trained using real-world data. Second, the data sizes in these studies were too small to be  
282 representative. We demonstrated that the ML-based models for predicting *VRE<sub>fm</sub>* can be  
283 applied as a clinical decision support tool by using the largest up-to-date datasets collected  
284 through the direct deposition method and various validation methods.

285 Identifying crucial predictive peaks in *VRE<sub>fm</sub>* classification may not be essential in  
286 clinical application; however, the specific combination of crucial predictive peaks would  
287 inspire further studies investigating the molecular mechanism of *VRE<sub>fm</sub>*. Typically, the *vanA*  
288 cluster is the most common mediator of vancomycin resistance in enterococci,<sup>49</sup> although many  
289 vancomycin resistance genes have been identified.<sup>50</sup> In brief, many factors together attribute to  
290 antibiotic resistance. Moreover, the complex mechanisms of antibiotic resistance would evolve  
291 in response to the selective pressures of their competitive environment (eg, antibiotic use).<sup>49</sup>  
292 Thus, identifying the important predictive peaks for *VRE<sub>fm</sub>* could help us understand the  
293 mechanism behind resistance. In this study, for example, peaks of *m/z* 6603, 6631, and 6635  
294 were found frequently for *VRE<sub>fm</sub>* (eTable 2 in the Supplement). The finding is consistent with

295 a previous study where Griffin et al. reported  $m/z$  6603 is specific for *vanB*-positive *VREfm*,  
296 while  $m/z$  6631 and 6635 are specifically found for *vanA*-positive *VREfm*.<sup>38</sup> These peaks are  
297 worthy of further identification in future investigations. Moreover, new antibiotics against  
298 *VREfm* can be developed based on these predictive peaks for *VREfm*.

299 Our ML models persistently performed well in 5-fold CV, time-wise internal validation,  
300 and external validation. Moreover, all the ML algorithms used in this study exhibited good  
301 performance (AUROC > 0.8). It could be explained that discriminating *VREfm* from *VSEfm*  
302 is generally achievable after adequate feature extraction and feature selection processes. In  
303 time-wise internal validation, we intended to simulate a prospective study for a model trained  
304 by the “past data” to analyze the “future data.” Based on the performance of time-wise internal  
305 validation, we concluded that the trained ML models could also perform well on the  
306 prospectively collected data, which are unseen in the training process. Previous study results  
307 differentiating *VREfm* from *VSEfm* by using MALDI-TOF MS spectra could not be  
308 generalized.<sup>23-25,38</sup> The inconsistent results could be because less features (<10) were used. A  
309 review article reported that peak-level reproducibility of MALDI-TOF mass is approximately  
310 80%.<sup>51</sup> The classification performance is compromised when essential peaks are few and  
311 happen to be absent on the mass spectra. In our study, the ML models performed stably when  
312 the included peaks were more than 100 (eFigure 4 in the Supplement). The steady and good  
313 performance of our ML models could be explained by the much more included peaks: when  
314 some of the essential peaks are not reproduced in the mass spectra, we can still use other  
315 alternative essential peaks to conduct an accurate classification. The number of essential peaks  
316 somehow compensated the insufficient reproducibility of MALDI-TOF mass. By contrast,  
317 regarding predicting *VREfm* for various specimens, we found that the RF-based model  
318 performed especially well in blood and sterile body fluids. The superior prediction performance  
319 could be attributed to the relatively fewer number of *VREfm* strains in blood and sterile body

320 fluids. Bacterial infection in blood or sterile body fluids is typically regarded as invasive  
321 infection.<sup>52</sup> Only a few *VREfm* strains (sequence type (ST)17, ST18, ST78, and ST203) cause  
322 invasive infections in blood or sterile body fluids according to the studies in Taiwan<sup>53</sup> and  
323 Ireland.<sup>54</sup> The nature of the classification problem would be more simple when the number of  
324 labels is fewer.

325

## 326 **Limitations**

327 This study has several limitations. First, although the models were evaluated using  
328 unseen external data from different medical centers, all the training data and testing data were  
329 collected from only 2 tertiary medical centers in Taiwan. Directly applying the ML models in  
330 hospitals of other areas or countries as well as in primary care institutes may not be appropriate.  
331 However, we believe that the method, but not the trained model, could be generalized.  
332 Although our ML models were validated comprehensively using 3 different approaches and  
333 the results show that the difference in MALDI-TOF mass spectra between *VREfm* and *VSEfm*  
334 can be distinguished through all the ML algorithms we used, we suggest others collecting their  
335 locally relevant data for training and validating the *VREfm* predicting model given that the  
336 epidemiology of *VREfm* could be fairly different site by site. Second, our primary goal was to  
337 develop and validate a practical and ready-to-use ML model in real-world practice. We found  
338 some crucial predictive peaks for *VREfm*; however, we did not confirm the identities for these  
339 peaks. It is worthy of identifying these peaks in further investigations. Third, we did not use  
340 the deep learning (DL) algorithm for predicting *VREfm*, although DL has been successful in  
341 the image classification or radiology field.<sup>32,33</sup> In this study, *VREfm* could be accurately  
342 predicted using several classic algorithms (ie, RF, SVM, and KNN) that require less resource  
343 and time in training and using models. Moreover, DL usually requires more training samples  
344 and is financially and computationally more expensive than classical ML algorithms.<sup>55</sup> DL

345 utility in analyzing MS data rather than image data could be another promising issue in the  
346 bioinformatics field. Fourth, no strain typing data were included. Thus, the molecular  
347 epidemiology of *VRE<sub>fm</sub>* used in this study is unknown.

348

### 349 **Conclusions**

350 We developed and validated robust ML models capable of discriminating *VRE<sub>fm</sub>* from  
351 *VSE<sub>fm</sub>* based on MALDI-TOF MS spectra. These models were especially good at detecting  
352 *VRE<sub>fm</sub>* causing invasive diseases. The accurate and rapid detection of *VRE<sub>fm</sub>* by using the ML  
353 models would facilitate more appropriate antibiotic prescription.

354

### 355 **Acknowledgments**

356 This manuscript was edited by Wallace Academic Editing.

357

### 358 **Author Contributions**

359 HYW, KPL, and CRC had full access to all the data in the study and take responsibility for the  
360 integrity of the data and the accuracy of data analysis. HYW, KPL, CRC, and YJT  
361 analyzed/interpreted the data, performed experiments, designed the study, and wrote the  
362 manuscript. HYW, CRC, YJT, JTH, TYL, THC, MHW, TPL, and JLL reviewed/edited the  
363 manuscript for important intellectual content and provided administrative, technical, or  
364 material support. JLL obtained funding and supervised the study.

365

### 366 **Funding**

367 This work was supported by Chang Gung Memorial Hospital (CMRPG3F1721,  
368 CMRPG3F1722, CMRPD3I0011) and the Ministry of Science and Technology, Taiwan

369 (MOST 107-2320-B-182A-021-MY3, MOST 108-2636-E-182-001, and MOST 107-2636-E-  
370 182-001).

371

372 **Competing interests**

373 The authors have no affiliations with or involvement in any organization or entity with any  
374 financial interest or non-financial interest in the subject matter or materials discussed in this  
375 manuscript.

376

377 **References**

- 378 1 Arias, C. A. & Murray, B. E. The rise of the Enterococcus: beyond vancomycin  
379 resistance. *Nat Rev Microbiol* **10**, 266-278, doi:10.1038/nrmicro2761 (2012).
- 380 2 Marra, A. R. *et al.* Nosocomial Bloodstream Infections in Brazilian Hospitals: Analysis  
381 of 2,563 Cases from a Prospective Nationwide Surveillance Study. *Journal of Clinical*  
382 *Microbiology* **49**, 1866-1871, doi:10.1128/JCM.00376-11 (2011).
- 383 3 Cetinkaya, Y., Falk, P. & Mayhall, C. G. Vancomycin-Resistant Enterococci. *Clinical*  
384 *Microbiology Reviews* **13**, 686-707, doi:10.1128/CMR.13.4.686 (2000).
- 385 4 Arias, C. A., Contreras, G. A. & Murray, B. E. Management of multidrug-resistant  
386 enterococcal infections. *Clin Microbiol Infect* **16**, 555-562, doi:10.1111/j.1198-  
387 743X.2010.03214.x (2010).
- 388 5 Leclercq, R., Derlot, E., Duval, J. & Courvalin, P. Plasmid-mediated resistance to  
389 vancomycin and teicoplanin in *Enterococcus faecium*. *N Engl J Med* **319**, 157-161,  
390 doi:10.1056/NEJM198807213190307 (1988).
- 391 6 Sahm, D. F. *et al.* In vitro susceptibility studies of vancomycin-resistant *Enterococcus*  
392 *faecalis*. *Antimicrobial Agents and Chemotherapy* **33**, 1588-1591,  
393 doi:10.1128/aac.33.9.1588 (1989).
- 394 7 Sader, H. S., Moet, G. J., Farrell, D. J. & Jones, R. N. Antimicrobial susceptibility of  
395 daptomycin and comparator agents tested against methicillin-resistant *Staphylococcus*  
396 *aureus* and vancomycin-resistant enterococci: trend analysis of a 6-year period in US  
397 medical centers (2005–2010). *Diagnostic Microbiology and Infectious Disease* **70**,  
398 412-416, doi:10.1016/j.diagmicrobio.2011.02.008 (2011).
- 399 8 Lodise, T. P., McKinnon, P. S., Tam, V. H. & Rybak, M. J. Clinical outcomes for  
400 patients with bacteremia caused by vancomycin-resistant enterococcus in a level 1  
401 trauma center. *Clin Infect Dis* **34**, 922-929, doi:10.1086/339211 (2002).
- 402 9 Ghanem, G., Hachem, R., Jiang, Y., Chemaly, R. F. & Raad, I. Outcomes for and Risk  
403 Factors Associated With Vancomycin-Resistant *Enterococcus faecalis* and  
404 Vancomycin-Resistant *Enterococcus faecium* Bacteremia in Cancer Patients. *Infection*  
405 *Control & Hospital Epidemiology* **28**, 1054-1059, doi:10.1086/519932 (2015).
- 406 10 Ozsoy, S. & Ilki, A. Detection of vancomycin-resistant enterococci (VRE) in stool  
407 specimens submitted for *Clostridium difficile* toxin testing. *Braz J Microbiol* **48**, 489-  
408 492, doi:10.1016/j.bjm.2016.12.012 (2017).
- 409 11 Balli, E. P., Venetis, C. A. & Miyakis, S. Systematic Review and Meta-Analysis of  
410 Linezolid versus Daptomycin for Treatment of Vancomycin-Resistant Enterococcal  
411 Bacteremia. *Antimicrobial Agents and Chemotherapy* **58**, 734-739,  
412 doi:10.1128/AAC.01289-13 (2014).
- 413 12 Crank, C. & O'Driscoll, T. Vancomycin-resistant enterococcal infections:  
414 epidemiology, clinical manifestations, and optimal management. *Infection and Drug*  
415 *Resistance*, doi:<http://dx.doi.org/10.2147/IDR.S54125> (2015).
- 416 13 CLSI. Performance Standards for Antimicrobial Susceptibility Testing. 27th ed. CLSI  
417 supplement M100. Wayne, PA: *Clinical and Laboratory Standards Institute* (2017).
- 418 14 Hrabak, J., Chudackova, E. & Walkova, R. Matrix-assisted laser desorption ionization-  
419 time of flight (maldi-tof) mass spectrometry for detection of antibiotic resistance  
420 mechanisms: from research to routine diagnosis. *Clin Microbiol Rev* **26**, 103-114,  
421 doi:10.1128/CMR.00058-12 (2013).
- 422 15 Idelevich, E. A., Sparbier, K., Kostrzewa, M. & Becker, K. Rapid detection of antibiotic  
423 resistance by MALDI-TOF mass spectrometry using a novel direct-on-target  
424 microdroplet growth assay. *Clin Microbiol Infect*, doi:10.1016/j.cmi.2017.10.016  
425 (2017).



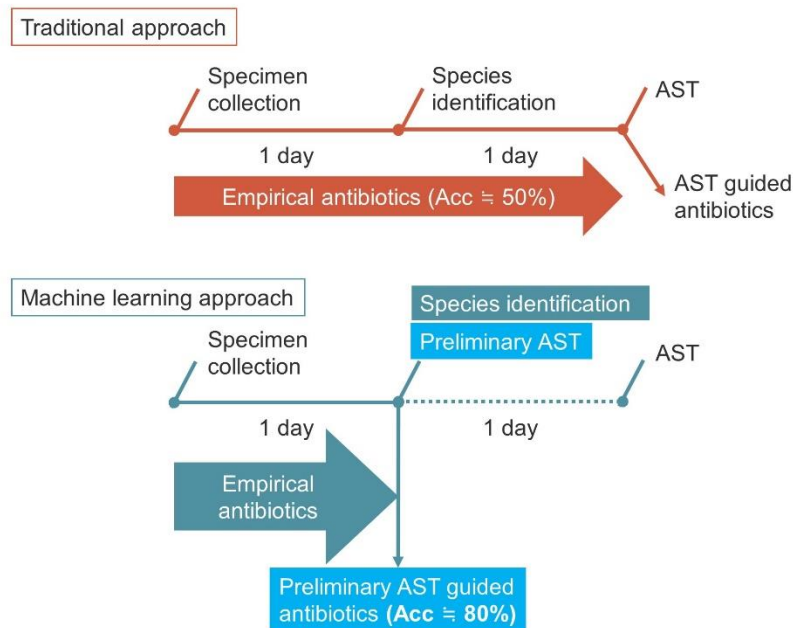
- 426 16 Suarez, S. *et al.* Ribosomal proteins as biomarkers for bacterial identification by mass  
427 spectrometry in the clinical microbiology laboratory. *J Microbiol Methods* **94**, 390-396,  
428 doi:10.1016/j.mimet.2013.07.021 (2013).
- 429 17 Wang, H.-Y. *et al.* Application of a MALDI-TOF analysis platform (ClinProTools) for  
430 rapid and preliminary report of MRSA sequence types in Taiwan. *PeerJ* **6**,  
431 doi:10.7717/peerj.5784 (2018).
- 432 18 Wang, H. Y. *et al.* Rapid Detection of Heterogeneous Vancomycin-Intermediate  
433 *Staphylococcus aureus* Based on Matrix-Assisted Laser Desorption Ionization Time-  
434 of-Flight: Using a Machine Learning Approach and Unbiased Validation. *Front*  
435 *Microbiol* **9**, 2393, doi:10.3389/fmicb.2018.02393 (2018).
- 436 19 Wang, H. Y. *et al.* A new scheme for strain typing of methicillin-resistant  
437 *Staphylococcus aureus* on the basis of matrix-assisted laser desorption ionization time-  
438 of-flight mass spectrometry by using machine learning approach. *PLoS One* **13**,  
439 e0194289, doi:10.1371/journal.pone.0194289 (2018).
- 440 20 Lopez-Fernandez, H. *et al.* Mass-Up: an all-in-one open software application for  
441 MALDI-TOF mass spectrometry knowledge discovery. *BMC Bioinformatics* **16**, 318,  
442 doi:10.1186/s12859-015-0752-4 (2015).
- 443 21 Lasch, P. *et al.* Insufficient discriminatory power of MALDI-TOF mass spectrometry  
444 for typing of *Enterococcus faecium* and *Staphylococcus aureus* isolates. *Journal of*  
445 *microbiological methods* **100**, 58-69, doi:10.1016/j.mimet.2014.02.015 (2014).
- 446 22 Wolters, M. *et al.* MALDI-TOF MS fingerprinting allows for discrimination of major  
447 methicillin-resistant *Staphylococcus aureus* lineages. *International journal of medical*  
448 *microbiology : IJMM* **301**, 64-68, doi:10.1016/j.ijmm.2010.06.002 (2011).
- 449 23 Burckhardt, I. & Zimmermann, S. Susceptibility Testing of Bacteria Using Maldi-Tof  
450 Mass Spectrometry. *Front Microbiol* **9**, 1744, doi:10.3389/fmicb.2018.01744 (2018).
- 451 24 Vrioni, G. *et al.* MALDI-TOF mass spectrometry technology for detecting biomarkers  
452 of antimicrobial resistance: current achievements and future perspectives. *Ann Transl*  
453 *Med* **6**, 240, doi:10.21037/atm.2018.06.28 (2018).
- 454 25 Kostrzewa, M., Sparbier, K., Maier, T. & Schubert, S. MALDI-TOF MS: an upcoming  
455 tool for rapid detection of antibiotic resistance in microorganisms. *Proteomics Clin*  
456 *Appl* **7**, 767-778, doi:<https://doi.org/10.1002/prca.201300042> (2013).
- 457 26 Witten, I. H., Frank, E., Hall, M. A. & Pal, C. J. *Data Mining: Practical machine*  
458 *learning tools and techniques*. (Morgan Kaufmann, 2016).
- 459 27 Lo-Ciganic, W.-H. *et al.* Evaluation of Machine-Learning Algorithms for Predicting  
460 Opioid Overdose Risk Among Medicare Beneficiaries With Opioid Prescriptions.  
461 *JAMA Network Open* **2**, doi:10.1001/jamanetworkopen.2019.0968 (2019).
- 462 28 Tseng, Y.-J. *et al.* Predicting breast cancer metastasis by using serum biomarkers and  
463 clinicopathological data with machine learning technologies. *International Journal of*  
464 *Medical Informatics*, doi:10.1016/j.ijmedinf.2019.05.003 (2019).
- 465 29 Kuppermann, N. *et al.* A Clinical Prediction Rule to Identify Febrile Infants 60 Days  
466 and Younger at Low Risk for Serious Bacterial Infections. *JAMA Pediatr*,  
467 doi:10.1001/jamapediatrics.2018.5501 (2019).
- 468 30 Norgeot, B. *et al.* Assessment of a Deep Learning Model Based on Electronic Health  
469 Record Data to Forecast Clinical Outcomes in Patients With Rheumatoid Arthritis.  
470 *JAMA Network Open* **2**, doi:10.1001/jamanetworkopen.2019.0606 (2019).
- 471 31 Karter, A. J. *et al.* Development and Validation of a Tool to Identify Patients With Type  
472 2 Diabetes at High Risk of Hypoglycemia-Related Emergency Department or Hospital  
473 Use. *JAMA Internal Medicine* **177**, doi:10.1001/jamainternmed.2017.3844 (2017).

- 474 32 Gulshan, V. *et al.* Development and Validation of a Deep Learning Algorithm for  
475 Detection of Diabetic Retinopathy in Retinal Fundus Photographs. *Jama* **316**,  
476 doi:10.1001/jama.2016.17216 (2016).
- 477 33 Hwang, E. J. *et al.* Development and Validation of a Deep Learning-Based Automated  
478 Detection Algorithm for Major Thoracic Diseases on Chest Radiographs. *JAMA Netw*  
479 *Open* **2**, e191095, doi:10.1001/jamanetworkopen.2019.1095 (2019).
- 480 34 Elfiky, A. A., Pany, M. J., Parikh, R. B. & Obermeyer, Z. Development and Application  
481 of a Machine Learning Approach to Assess Short-term Mortality Risk Among Patients  
482 With Cancer Starting Chemotherapy. *JAMA Netw Open* **1**, e180926,  
483 doi:10.1001/jamanetworkopen.2018.0926 (2018).
- 484 35 Lin, W. Y. *et al.* Predicting post-stroke activities of daily living through a machine  
485 learning-based approach on initiating rehabilitation. *Int J Med Inform* **111**, 159-164,  
486 doi:10.1016/j.ijmedinf.2018.01.002 (2018).
- 487 36 Wang, H. Y. *et al.* Cancers Screening in an Asymptomatic Population by Using  
488 Multiple Tumour Markers. *PLoS One* **11**, e0158285,  
489 doi:10.1371/journal.pone.0158285 (2016).
- 490 37 Nakano, S. *et al.* Differentiation of vanA-positive *Enterococcus faecium* from vanA-  
491 negative *E. faecium* by matrix-assisted laser desorption/ionisation time-of-flight mass  
492 spectrometry. *Int J Antimicrob Agents* **44**, 256-259,  
493 doi:10.1016/j.ijantimicag.2014.05.006 (2014).
- 494 38 Griffin, P. M. *et al.* Use of matrix-assisted laser desorption ionization-time of flight  
495 mass spectrometry to identify vancomycin-resistant enterococci and investigate the  
496 epidemiology of an outbreak. *J Clin Microbiol* **50**, 2918-2931,  
497 doi:10.1128/JCM.01000-12 (2012).
- 498 39 Huang, T. S. *et al.* Evaluation of a matrix-assisted laser desorption ionization-time of  
499 flight mass spectrometry assisted, selective broth method to screen for vancomycin-  
500 resistant enterococci in patients at high risk. *PLoS One* **12**, e0179455,  
501 doi:10.1371/journal.pone.0179455 (2017).
- 502 40 Corrigan-Curay, J., Sacks, L. & Woodcock, J. Real-World Evidence and Real-World  
503 Data for Evaluating Drug Safety and Effectiveness. *Jama* **320**,  
504 doi:10.1001/jama.2018.10136 (2018).
- 505 41 Bossuyt, P. M. *et al.* STARD 2015: an updated list of essential items for reporting  
506 diagnostic accuracy studies. *BMJ* **351**, h5527, doi:10.1136/bmj.h5527 (2015).
- 507 42 Collins, G. S., Reitsma, J. B., Altman, D. G. & Moons, K. G. Transparent reporting of  
508 a multivariable prediction model for individual prognosis or diagnosis (TRIPOD): the  
509 TRIPOD statement. *BMJ* **350**, g7594, doi:10.1136/bmj.g7594 (2015).
- 510 43 Saeys, Y., Inza, I. & Larranaga, P. A review of feature selection techniques in  
511 bioinformatics. *Bioinformatics* **23**, 2507-2517, doi:10.1093/bioinformatics/btm344  
512 (2007).
- 513 44 Cochran, W. G. The Comparison of Percentages in Matched Samples. *Biometrika* **37**,  
514 doi:10.2307/2332378 (1950).
- 515 45 McNemar, Q. Note on the sampling error of the difference between correlated  
516 proportions or percentages. *Psychometrika* **12**, 153-157, doi:10.1007/BF02295996  
517 (1947).
- 518 46 Benjamini, Y. & Hochberg, Y. Controlling the False Discovery Rate: A Practical and  
519 Powerful Approach to Multiple Testing. *Journal of the Royal Statistical Society: Series*  
520 *B (Methodological)* **57**, 289-300, doi:[https://doi.org/10.1111/j.2517-](https://doi.org/10.1111/j.2517-6161.1995.tb02031.x)  
521 [6161.1995.tb02031.x](https://doi.org/10.1111/j.2517-6161.1995.tb02031.x) (1995).

- 522 47 DeLong, E. R., DeLong, D. M. & Clarke-Pearson, D. L. Comparing the Areas under  
523 Two or More Correlated Receiver Operating Characteristic Curves: A Nonparametric  
524 Approach. *Biometrics* **44**, doi:10.2307/2531595 (1988).
- 525 48 Mather, C. A., Werth, B. J., Sivagnanam, S., SenGupta, D. J. & Butler-Wu, S. M. Rapid  
526 Detection of Vancomycin-Intermediate Staphylococcus aureus by Matrix-Assisted  
527 Laser Desorption Ionization-Time of Flight Mass Spectrometry. *J Clin Microbiol* **54**,  
528 883-890, doi:10.1128/JCM.02428-15 (2016).
- 529 49 Miller, W. R., Munita, J. M. & Arias, C. A. Mechanisms of antibiotic resistance in  
530 enterococci. *Expert Review of Anti-infective Therapy* **12**, 1221-1236,  
531 doi:10.1586/14787210.2014.956092 (2014).
- 532 50 Lebreton, F. *et al.* D-Ala-d-Ser VanN-type transferable vancomycin resistance in  
533 Enterococcus faecium. *Antimicrob Agents Chemother* **55**, 4606-4612,  
534 doi:10.1128/AAC.00714-11 (2011).
- 535 51 Croxatto, A., Prod'hom, G. & Greub, G. Applications of MALDI-TOF mass  
536 spectrometry in clinical diagnostic microbiology. *FEMS microbiology reviews* **36**, 380-  
537 407, doi:10.1111/j.1574-6976.2011.00298.x (2012).
- 538 52 Lee, J. H. *et al.* Etiology of invasive bacterial infections in immunocompetent children  
539 in Korea (1996-2005): a retrospective multicenter study. *J Korean Med Sci* **26**, 174-  
540 183, doi:10.3346/jkms.2011.26.2.174 (2011).
- 541 53 Kuo, A. J. *et al.* Vancomycin-resistant Enterococcus faecium at a university hospital in  
542 Taiwan, 2002-2015: Fluctuation of genetic populations and emergence of a new  
543 structure type of the Tn1546-like element. *J Microbiol Immunol Infect* **51**, 821-828,  
544 doi:<https://doi.org/10.1016/j.jmii.2018.08.008> (2018).
- 545 54 Ryan, L. *et al.* Epidemiology and molecular typing of VRE bloodstream isolates in an  
546 Irish tertiary care hospital. *J Antimicrob Chemother* **70**, 2718-2724,  
547 doi:<https://doi.org/10.1093/jac/dkv185> (2015).
- 548 55 Liu, P., Choo, K.-K. R., Wang, L. & Huang, F. SVM or deep learning? A comparative  
549 study on remote sensing image classification. *Soft Computing* **21**, 7053-7065,  
550 doi:<https://doi.org/10.1007/s00500-016-2247-2> (2016).
- 551  
552

## 553 Figure legends

Figure 1(a)



554

555 **Figure 1(a). Scheme of using the VRE<sub>fm</sub> Model.** We plotted a timeline of bacterial culture

556 test in current clinical microbiology laboratory (i.e., traditional approach) and a

557 modified timeline when the VRE<sub>fm</sub> model is incorporated (i.e., machine learning

558 approach). In the traditional approach, specimens are collected for bacterial culture

559 test. One day is usually needed for growth of a single colony for species

560 identification (by MALDI-TOF MS). Antibiotics susceptibility test (AST) of

561 vancomycin for VRE<sub>fm</sub> will cost another day to report. By contrast, in the machine

562 learning approach, the VRE<sub>fm</sub> model can provide preliminary AST at the time when

563 bacterial species is identified by MALDI-TOF MS. For treating VRE<sub>fm</sub>, the machine

564 learning approach can improve accuracy of antibiotics use by around 30% (from

565 50% accuracy of empirical antibiotics use in the traditional approach to 80%

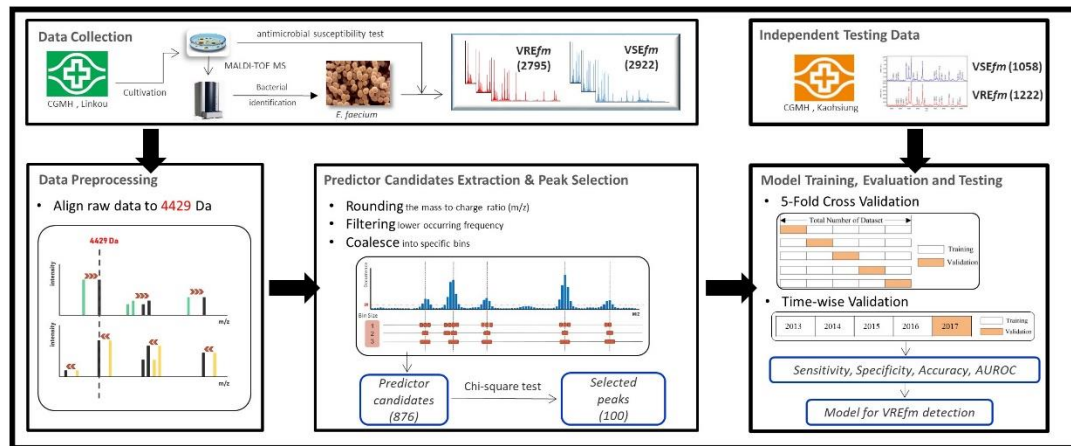
566 accuracy of preliminary AST provided by the machine learning approach).

567 Meanwhile, the turn-around-time of bacterial culture test can be reduced to one day,

568 which is 50% reduction.

569

Figure 1(b)



570

571 **Figure 1(b). Schematic Illustration of the Study Design.** We developed and validated a VRE<sub>fm</sub>

572 prediction model. The study included several steps, namely data collection, data

573 preprocessing, predictor candidate extraction and important predictor selection, model

574 training, evaluation, and testing. In data collection, data were obtained from 2 tertiary

575 medical centers (Linkou and Kaohsiung branches of CGMH). The data included mass

576 spectra and results of the vancomycin susceptibility test of *E. faecium*. Data from the CGMH

577 Linkou branch were used for model training and validation, while data from the CGMH

578 Kaohsiung branch served as an independent testing data. In the steps of data preprocessing

579 and predictor candidate extraction and important predictor selection, a specific set of crucial

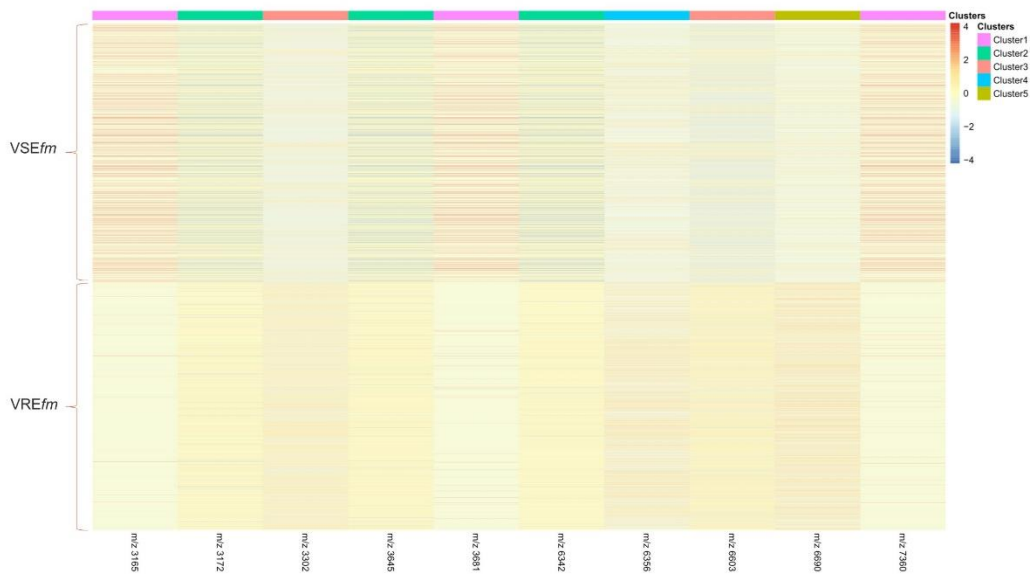
580 predictors would be used for model training. K-fold, time-wise CV, and external validation

581 were used to confirm the models' robustness. The VRE<sub>fm</sub> prediction model can detect

582 VRE<sub>fm</sub> accurately at least 1 day earlier than the current method.

583

Figure 2



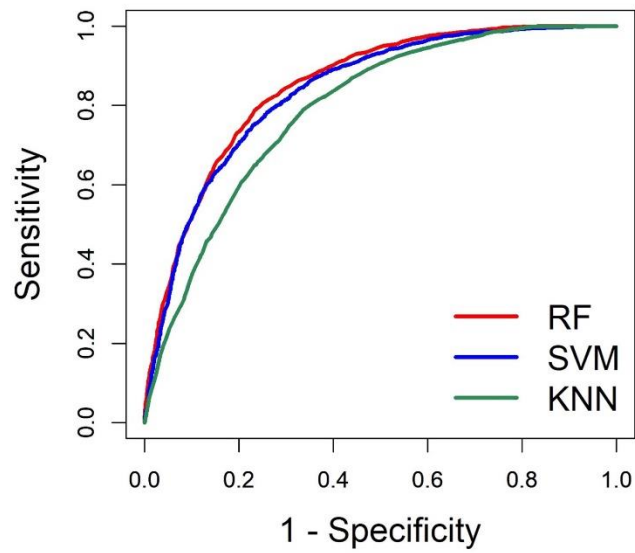
584

585 **Figure 2. Heat map.** We selected top 10 discriminative peaks by chi-square testing the occurrence  
586 frequency of peaks in *VREfm* and *VSEfm*. The heat map was plotted based on the hierarchical  
587 clustering of all the *VREfm* and *VSEfm* isolates from the CGMH Linkou branch. Rows  
588 represent the isolates, and columns represent the top 10 discriminative peaks. The values in  
589 the heat map represent the MS spectral intensity which was  $\log_{10}$ -normalized and z-score  
590 standardized. Red color indicates relatively higher peak intensity while blue color indicates  
591 lower peak intensity. The isolates are grouped into 5 clusters. *VREfm* and *VSEfm* isolates can  
592 be visually differentiated by using the top 10 discriminative peaks.

593



Figure 3(a)

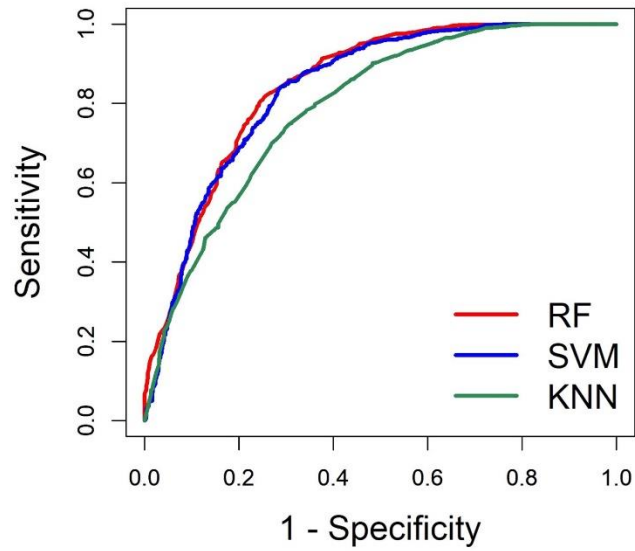


594

595 **Figure 3(a). ROC Curves for Different Algorithms in Terms of Linkou 5-Fold CV**

596

Figure 3(b)



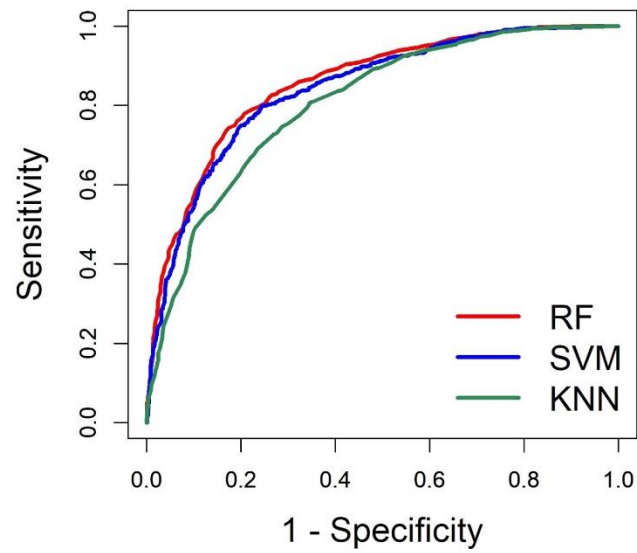
597

598 **Figure 3(b). ROC Curves for Different Algorithms in Terms of Time-Wise Validation**

599



Figure 3(c)

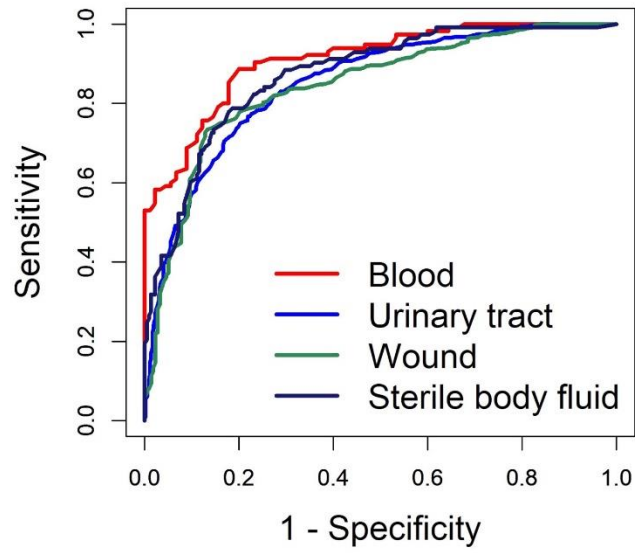


600

601 **Figure 3(c). ROC Curves for Different Algorithms in Terms of External Validation**

602

Figure 3(d)



603

604 **Figure 3(d). ROC Curves for the RF-Based VRE<sub>fm</sub> Model With Different Types of**

605 **Specimens**

606

607 **Table 1. Performance of VRE<sub>fm</sub> Prediction Models in Terms of k-Fold CV, Time-Wise**  
 608 **Validation, and External Validation**

AUROC	RF	SVM	KNN
5-fold CV	0.8495 (0.8397, 0.8594)	0.8367 (0.8264, 0.8471)	0.7908 (0.7792, 0.8024)
Time-wise validation	0.8463 (0.8273, 0.8654)	0.8368 (0.8169, 0.8566)	0.7908 (0.7690, 0.8127)
External validation	0.8553 (0.8399, 0.8706)	0.8407 (0.8246, 0.8569)	0.8050 (0.7872, 0.8227)
Accuracy			
5-fold CV	0.7769 (0.7660, 0.7878)	0.7610 (0.7499, 0.7721)	0.7248 (0.7131, 0.7364)
Time-wise validation	0.7840 (0.7640, 0.8039)	0.7815 (0.7615, 0.8016)	0.7228 (0.7011, 0.7445)
External validation	0.7855 (0.7687, 0.8024)	0.7781 (0.7610, 0.7951)	0.7355 (0.7174, 0.7536)
Sensitivity			
5-fold CV	0.8054 (0.7951, 0.8517)	0.7826 (0.7719, 0.7934)	0.7873 (0.7767, 0.7980)
Time-wise validation	0.8153 (0.7965, 0.8341)	0.8415 (0.8238, 0.8592)	0.7491 (0.7281, 0.7702)
External validation	0.7791 (0.7620, 0.7961)	0.7954 (0.7789, 0.8120)	0.8044 (0.7881, 0.8207)
Specificity			
5-fold CV	0.7497 (0.7384, 0.7609)	0.7403 (0.7289, 0.7517)	0.6649 (0.6526, 0.6772)
Time-wise validation	0.7477 (0.7266, 0.7688)	0.7120 (0.6900, 0.7340)	0.6922 (0.6698, 0.7146)
External validation	0.7930 (0.7764, 0.8096)	0.7580 (0.7405, 0.7756)	0.6560 (0.6365, 0.6755)

609

610 AUROC, area under the receiver operating characteristic curve.

611

612 **Table 2. Performance of the RF-Based VRE<sub>fm</sub> Detection Model With Different Types of**  
613 **Specimens in Terms of External Validation**

Metrics	Type			
	Blood	Urinary tract	Sterile body fluid	Wound
AUROC	0.9103 (0.8727, 0.9480)	0.8494 (0.8258, 0.8731)	0.8714 (0.8321, 0.9106)	0.8432 (0.8121, 0.8743)
Accuracy	0.8488 (0.7997, 0.8978)	0.7743 (0.7482, 0.8004)	0.8077 (0.7657, 0.8497)	0.7740 (0.7436, 0.8043)
Sensitivity	0.8870 (0.8436, 0.9303)	0.7672 (0.7409, 0.7936)	0.7788 (0.7345, 0.8230)	0.7339 (0.7018, 0.7659)
Specificity	0.8000 (0.7452, 0.8548)	0.7805 (0.7547, 0.8063)	0.8222 (0.7815, 0.8630)	0.8676 (0.8430, 0.8922)

614

615